THE ASTRONOMICAL JOURNAL, 121:2420–2430, 2001 May

GAS MASS FRACTIONS AND THE EVOLUTION OF LOW SURFACE BRIGHTNESS DWARF GALAXIES

JAMES M. SCHOMBERT
Department of Physics, University of Oregon, Eugene, OR 97403; js@abyss.uoregon.edu
STACY S. MCGAUGH
Department of Astronomy, University of Maryland, College Park, MD 20742; ssm@astro.umd.edu
AND
JO ANN EDER
Arecibo Observatory,[1] P. O. Box 995, Arecibo, PR 00612; eder@naic.edu
Received 2000 November 12; accepted 2001 January 23

ABSTRACT

The optical and H I properties are presented for a sample of low surface brightness (LSB) dwarf galaxies, cataloged from the Second Palomar Sky Survey. Gas mass fractions for LSB dwarfs reach the highest levels of any know galaxy type ($f_g = 95\%$), confirming that their low stellar densities are due to inefficient conversion of gas mass into stellar mass. Comparison with star formation models indicates that the blue optical colors of LSB dwarfs are not due to low metallicity or to recent star formation and can only be explained by a dominant stellar population less than 5 Gyr in mean age. If star formation occurs in OB complexes, as in normal galaxies, then LSB dwarfs must undergo weak bursts traveling over the extent of the galaxy to maintain their LSB nature, which contributes to their irregular morphological appearance.

Key words: galaxies: dwarf — galaxies: evolution — galaxies: stellar content

1. INTRODUCTION

Dwarf galaxies are important to our understanding of galaxy formation and evolution, because they are the smallest star-forming units at the time of galaxy formation. Under the bottom-up scenarios of galaxy formation (Lake 1990; Baugh, Cole, & Frenk 1996), dwarf galaxies are the building blocks of the entire Hubble sequence, and thus the study of dwarf galaxies is a look at the fossil remnants of the early universe. In addition, dwarfs are extremely rich in dark matter as compared to the amount of known baryons calculated from starlight and neutral gas emission (Ashman 1992; Carignan & Purton 1998). They serve as laboratories to test dark matter candidates and to study the formation and evolution of the dark matter component in galaxies. Regardless of their cosmological importance, however, the primary role of dwarf galaxies is that they present us with extreme limits with respect to star formation and stellar populations in galaxies. Much as a psychologist studies extreme behavior to better understand normal behavior, the study of dwarf galaxies leads to clues into the star formation processes that are found in all galaxies, from dwarf to giant, from quiescent to starburst.

The key to the star formation history of any galaxy and to its subsequent evolution is its gas supply. Whether the gas supply is converted completely into stars immediately after formation, as in ellipticals, or whether the gas supply remains dispersed until a dynamic event increases the number of cloud collisions, as in a tidally induced starburst, the gas mass fraction, f_g, is the primary parameter for quantifying the evolutionary state of a galaxy. A galaxy's chemical and photometric evolution closely follows the gas consumption rate. For example, Bell & de Jong (2000) demonstrate that the metallicity of spirals follows a simple closed-box chemical evolution model and also predicts the colors of the underlying stellar population. With respect to low surface brightness (LSB) galaxies, van den Hoek et al. (2000) find that a majority of LSB disks can be explained by an exponentially decreasing star formation rate, ending with present-day gas fractions near 0.5.

Historically, gas-rich galaxies have been divided into two types, disk galaxies and dwarf galaxies. Disk galaxies are brighter and higher in surface brightness and have dominated our studies of the star formation process. In contrast, dwarf galaxies are fainter and lower in surface brightness, making their detection and inclusion in galaxy catalogs problematic. In the last decade, new galaxy catalogs (Schombert & Bothun 1988; Impey et al. 1996) have widened our range of central surface brightnesses to include new extremes in low stellar densities (i.e., LSB). The common interpretation is that these systems have had, in the past, very low rates of star formation (de Blok & van der Hulst 1998), and thus there is the expectation that LSB galaxies should be rich in gas compared to their stellar mass. This was confirmed by McGaugh & de Blok (1997, hereafter MdB) in a study of a large sample of disk galaxies over a range of surface brightnesses. They found that there is a strong correlation between a galaxy's gas supply and its stellar density, such that galaxies with the lowest surface brightness had the largest $M_{\rm H\,I}/L$ and f_g ratios. The gas fractions found by MdB also indicated that LSB galaxies have the potential to become extremely bright, high surface brightness (HSB) objects if some process increases the efficiency of star formation and rapidly uses the supply of gas (e.g., a tidal interaction). The discovery of star-forming dwarf populations in the field (Driver, Windhorst, & Griffiths 1995; Schade et al. 1996) and in distant clusters (Rakos, Odell, & Schombert 1997) makes an investigation into nearby quiescent dwarfs timely.

The correlations found for disk galaxies have never been extended to dwarf galaxies, primarily because of a lack of a uniform sample of gas-rich, LSB dwarfs. The purpose of this paper is to undertake an analysis of the LSB dwarfs from

[1] The Arecibo Observatory is part of the National Astronomy and Ionosphere Center, which is operated by Cornell University under contract with the National Science Foundation.

the PSS II survey similar to that performed by MdB on LSB disks and to compare the results to the correlations found for all types of disk galaxies. The dwarf sample used herein is based on a visual search of Second Palomar Sky Survey plates (Eder et al. 1989; Schombert, Pildis, & Eder 1997) parallel to searches for large LSB galaxies (Schombert & Bothun 1988; Schombert et al. 1992). This search was performed primarily for a study on biased galaxy formation, but optical and H I data are available for most of the dwarfs. The optical data for that sample were presented in Pildis, Schombert, & Eder (1997). The H I data are presented in Eder & Schombert (2000) and form the core of the analysis in this study.

2. OBSERVATIONS

The data for this paper are based on Second Palomar Sky Survey (PSS II; see Reid et al. 1991) plates cataloged in Schombert et al. (1997). The PSS II differed from the original sky survey in that the latest Kodak IIIa plates, which have greater resolution and depth than the original survey's 103a emulsions (250 lines mm^{-1} vs. 80 lines mm^{-1}), were used. The plates used for the dwarf catalog are A- or B-grade, selected for good surface brightness depth and covering declination zones of the sky that can be observed with the 305 m Arecibo radio telescope.

Dwarf candidates from the catalog were observed for the H I line at 21 cm with the Arecibo 305 m telescope during the 1992 and 1993 observing seasons. All observations were made with the 21 cm dual-circular feed positioned to provide a maximum gain (8 Km Jy^{-1}) at 1400 MHz. Total velocity coverage of 8000 km s^{-1} at a velocity resolution of 8.6 km s^{-1} was used. The observations were centered on 4000 km s^{-1}, avoiding detection of the strong Galactic hydrogen signal on the low-velocity end, and extended to 8120 km s^{-1}. The H I observations are reported in Eder & Schombert (2000).

Successful detections were later selected for follow-up CCD imaging on the Hiltner 2.4 m telescope located at Michigan-Dartmouth-MIT (MDM) Observatory. We obtained images using either a Thomson 400×576 pixel CCD ($0''.25$ $pixel^{-1}$) or a Ford-Loral 2048×2048 pixel CCD binned 3×3 ($0''.51$ $pixel^{-1}$), with minimal exposure times of 25 minutes in Johnson V and 15 minutes in Johnson I. The optical data (luminosities, colors, scale lengths, and surface brightnesses) are presented in Pildis et al. (1997).

In addition, data on ordinary spirals were extracted from two surveys, Courteau (1996) and de Jong (1996), for comparison with the LSB dwarf data. The Courteau survey was primarily focused on Sc galaxies, as probes to the Tully-Fisher relation, presenting CCD and H I observations of 189 galaxies. The CCD observations were obtained in B and R, but a simple linear transformation converts the R magnitudes to I to match our LSB dwarf luminosities. The de Jong sample consists of a range of spiral types greater than $2'$ in diameter and undisturbed in their morphology, selected from the UGC and imaged at $BVRIK$. H I parameters were obtained from a variety of sources in the literature using NED.

All distance-related values in this paper use values of $H_0 = 75$ km s^{-1} Mpc^{-1}, $\Omega_0 = 0.2$, a Virgo central velocity of 977 km s^{-1} and a Virgo infall of 300 km s^{-1}. The data used for this study are available at the LSB dwarf web site (www.zebu.uoregon.edu/~js).

3. DISCUSSION

3.1. *Optical Properties*

The optical properties of the PSS II dwarf sample are presented in Pildis et al. (1997). Unless specifically mentioned, all luminosities are I-band values and scale lengths are measured in I-band images. The choice of I-band values is made to minimize the error in calculating stellar mass from optical luminosities. Studies by stellar population models (Worthey 1994) show that M_*/L varies with time and star formation rate as a function of wavelength, but it is most stable in the far-red because of that band's distance in wavelength from the region around the 4000 Å break. Thus, I-band measurements (1) provide a more accurate estimate of the stellar mass of a galaxy than bluer passbands, (2) obtain a luminosity measure that varies less with recent star formation than bluer passbands, and (3) allow determination of structural parameters (such as scale length) which are less distorted by recent star formation events or dust. Although the I band is a difficult bandpass to observe, because of a bright background from atmospheric OH emission, gray and bright time at many intermediate-size telescopes is much more accessible than dark time, allowing long exposure times at bandpasses where the moonlight has a minor contribution.

To place the LSB dwarf sample in context with respect to disk galaxies, we have selected two comparison samples: the study of regular spirals by de Jong (1996) and a study of Sc galaxies by Courteau (1996). One advantage to using the Courteau Sc disks and de Jong spirals is that both samples were constructed using morphological criteria. The Courteau Sc sample was sorted from the NGC/UGC for late-type galaxies that display clear Sc-type spiral structure and rotational symmetry specifically so as to be homogeneous, for a study of the Tully-Fisher relation in late-type galaxies. While many of the Courteau objects are low in luminosity and small in size, they are not dwarflike in their appearance. The de Jong spirals were selected from the UGC with an emphasis on an undisturbed disklike appearance and, in this regard, complement Courteau's Sc sample by covering a larger range of disk Hubble types (from Sa to Sm).

The PSS II dwarf galaxy sample was chosen for two primary characteristics: dwarflike (i.e., irregular) morphology and low surface brightness (see Schombert et al. 1997). The morphology criterion was introduced to maximize the cataloging of low-mass objects in order to test theories of biased galaxy formation, the original goal of the project, under the assumption that all low-mass objects have an irregular appearance. This is not always the case (e.g., dwarf ellipticals), but this criterion has the added advantage of increasing the number of gas-rich dwarf galaxies in the sample and the probability of detection at 21 cm. The low surface brightness nature of the sample is due to the fact that any search for uncataloged galaxies will necessarily be limited by the depth of the survey material. Increased depth does not increase the detection of HSB objects, which are already cataloged unless just below the angular-size threshold. The greater sensitivity of the PSS II plate material produces an automatic bias toward LSB galaxies that were once too diffuse to be visually detected and now have better contrast and, therefore, higher visibility.

In a morphological sense, the de Jong and Courteau samples are diametric opposites of the PSS II dwarf sample. Whereas the disk samples are selected for their regularity in

spiral pattern, the LSB dwarfs are selected with an emphasis on their irregularity. The regularity of morphology should reflect the star formation history of the galaxy, i.e., a regular pattern in the disk sample evolves from the ordered motions of a density wave and, in contrast, the irregular nature of the LSB dwarfs represents a chaotic history of star formation. In addition, we can also compare the LSB dwarfs with the dwarf sample of Patterson & Thuan (1996, hereafter PT), a sample of galaxies selected from the UGC by morphology in a similar manner to the PSS II sample and also imaged at I.

A summary of the optical properties of the four samples is found in Figure 1: histograms of absolute magnitude (M_T^I), central surface brightness (μ_0^I), and scale length (α). These values are taken directly from Pildis et al. (1997) and MdB. The Courteau Sc sample was converted from R-band data using his $B-R$ values and a linear extrapolation to $R-I$ ($\langle R-I\rangle = 0.5$ for late-type galaxies). Absolute luminosities are based on the total magnitude of the galaxy (integrated curves of growth). Central surface brightness and scale length are based on exponential fits to the surface brightness profiles. Almost all the dwarf galaxies in this sample are well described by an exponential surface brightness profile. For objects with central concentrations (bulgelike cores), the profile fit was made to the linear region only, but the total magnitude includes the core luminosity. Given the extreme late-type nature of the samples, the core contribution is, in any case, very minor.

There are several key points to note from the histograms. One is that there is significant overlap in all of the optical parameters among the four samples. In other words, there is no single property of a galaxy whereby one could divide dwarfs from ordinary disk galaxies. The de Jong and Courteau samples have similar mean luminosities ($\langle M_T^I\rangle = -21.2$), which is much higher than the LSB or PT dwarf samples ($\langle M_T^I\rangle = -17.4$). This is not surprising, because spiral galaxies are known to have high rates of star formation, often covering most of their disk area, resulting in more stellar mass and therefore in higher central surface brightnesses. Surface brightness is not directly correlated with total luminosity, as can be seen from the distribution of the de Jong disk total magnitudes (de Jong 1996; see also Driver & Cross 2000). The LSB dwarf sample displays a fairly sharp cutoff in luminosity at $M_T^I = -19$, despite the fact that only morphology and surface brightness were used to select the sample.

The trend of central surface brightness in each sample is as expected. The LSB dwarfs have a low mean central surface brightness ($\langle \mu_0\rangle = 21.8$), although the de Jong disk sample overlaps the LSB dwarf sample (there are several

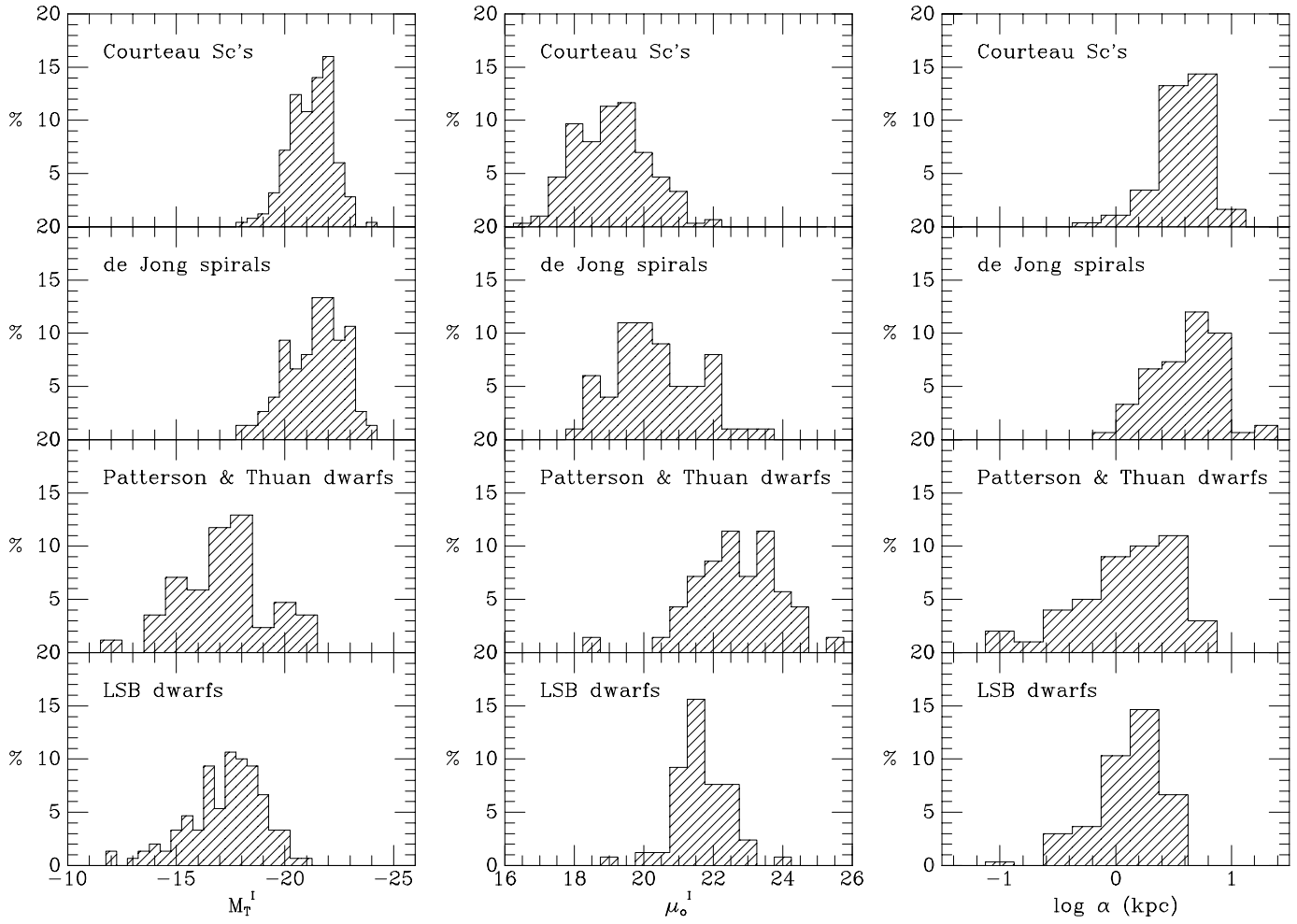

FIG. 1.—Histograms of total luminosity (M_T^I), central surface brightness (μ_0^I), and scale length (α) for the Courteau sample of Sc galaxies, the de Jong sample of ordinary spirals, the Patterson & Thuan UGC dwarf sample, and the LSB dwarf sample. The LSB dwarfs define a low-luminosity, low surface brightness, and small scale length sample of galaxies.

Sd- and Sm-class spirals in the de Jong sample). The PT dwarf sample has a similar distribution with a slightly fainter mean μ_0. The Courteau Sc sample has a brighter mean μ_0 ($\langle\mu_0\rangle = 19.0$), but the range is quite broad.

The histograms of scale length, α, are intriguing in that the de Jong disk and Courteau Sc sample have identical distributions, despite having reached their optical appearances by very different star formation histories (based on the final morphology and central surface brightness). This leads us to conclude that disk galaxies have the same range of sizes and masses and that Hubble class is imposed on disk galaxy structure by a set of parameters only weakly linked to the structural ones (angular momentum, environment, etc.; see Zaritsky 1993). The LSB and PT dwarfs have much lower values of α, with a cutoff at 3 kpc. In fact, size distribution is perhaps the most accurate method of distinguishing dwarf from ordinary galaxies when the mass is unknown (see Schombert et al. 1995).

3.2. H I *Properties*

It is often stated that LSB galaxies are gas-rich, which is loosely defined to mean that they have high amounts of neutral hydrogen relative to their optical luminosities. It should be noted that to state that the LSB dwarf sample is gas-rich does not imply that they have high H I masses. The distribution of H I masses (calculated from the total H I flux using the prescription of Giovanelli & Haynes 1988) is shown in Figure 2, along with the H I mass distribution of the de Jong spiral, Courteau Sc, and PT dwarf samples. The LSB dwarf distribution has a low mean value [$\langle M_{\rm H\,I}\rangle = 10^9 M_\odot$ compared to the $\langle M_{\rm H\,I}\rangle = (8 \times 10^9) M_\odot$ for the disk samples], with a long tail toward low H I masses. It is important to note that dwarfs selected by optical characteristics, such as size, are also dwarfs in terms of H I mass (see Eder & Schombert 2000).

The dwarfs in Figure 2 with H I masses less than $10^8\ M_\odot$ are of interest to galaxy population studies because there is some suggestion of a steepening of the H I mass function below $10^7\ M_\odot$ (Schneider, Spitzak, & Rosenberg 1998; Zwaan et al. 1997). There is no correlation between H I mass and surface brightness (Pildis et al. 1997); however, none of the $M_{\rm H\,I} < 10^8\ M_\odot$ dwarfs have central surface brightnesses brighter than $\mu_0^I = 21$ (approximately $\mu_0^B = 22.5$). This implies that low H I mass objects are underrepresented in our catalogs, because of the catalogs' bias toward high surface brightnesses objects, and that LSB, low H I mass galaxies have gone undetected in optical surveys (Schneider & Schombert 2000).

The distribution of the H I mass-to-luminosity ratio ($M_{\rm H\,I}/L$) is shown in the middle panel of Figure 2. The disk samples cover the same range ($0.03 \le M_{\rm H\,I}/L \le 5$); however, the Sc sample has a slightly higher mean

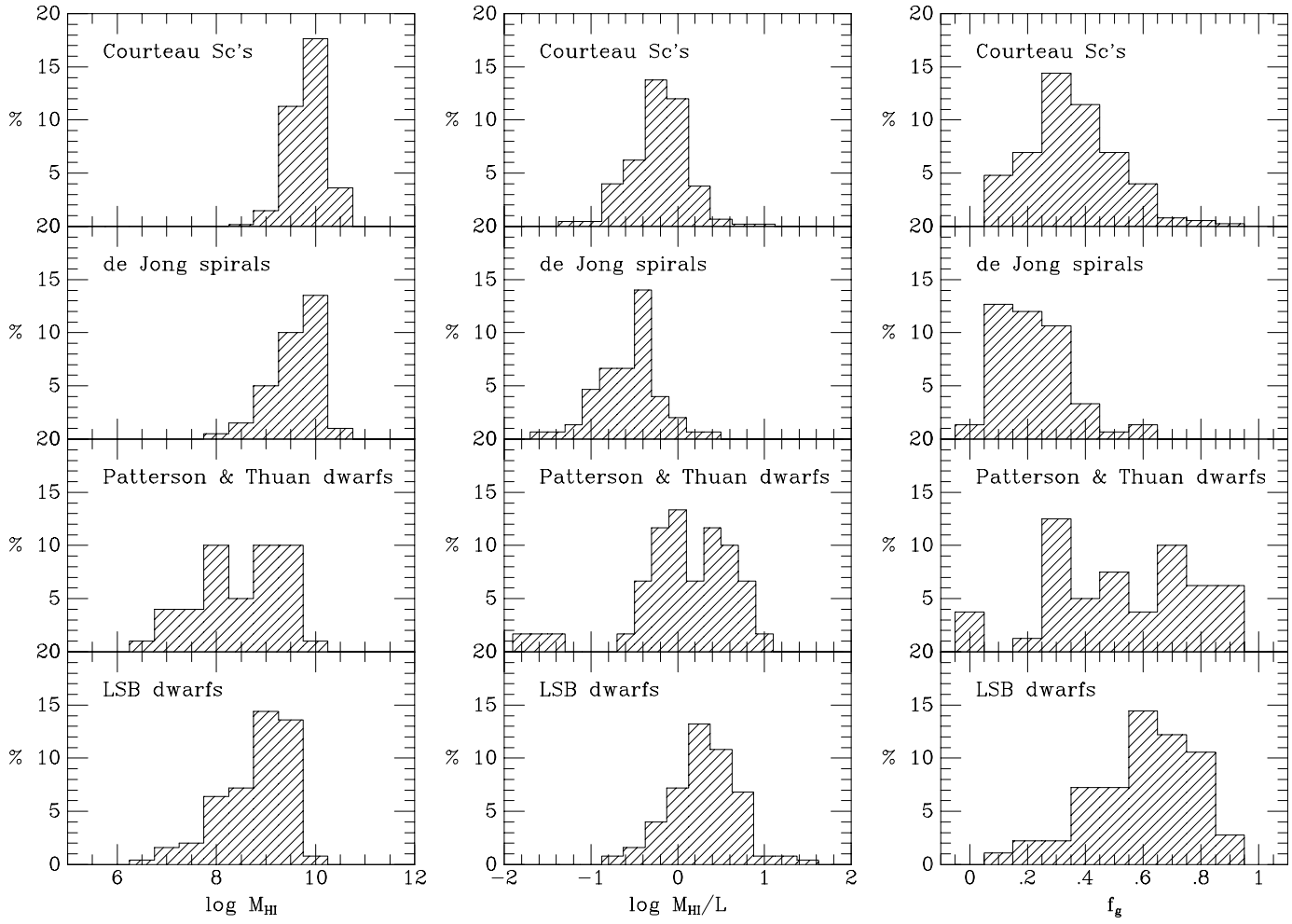

FIG. 2.—Histograms of H I mass, H I mass-to-light ratio ($M_{\rm H\,I}/L$), and gas mass fraction (f_g). While LSB dwarfs are low in total gas mass, their gas fractions are much higher than those of the spirals samples.

($\langle M_{\rm H\,I}/L\rangle = 0.8$) than the de Jong spirals, reflecting the known dependence of $M_{\rm H\,I}/L$ on Hubble type. The LSB dwarf sample has the highest mean values of $M_{\rm H\,I}/L$ ($\langle M_{\rm H\,I}/L\rangle = 3$), reflecting the increasing importance of neutral hydrogen to the baryonic content of these galaxies (see discussion in § 3.4). Matthews, van Driel, & Gallagher (1997) isolated a similar sample of high-$M_{\rm H\,I}/L$ galaxies, also selected from late-type galaxies, and the LSB dwarf sample shares many characteristics with their galaxies.

The relationship between stellar mass and gas mass is shown in Figure 3. As discussed in § 3.1, the luminosity of a galaxy at 9000 Å is an excellent measure of the number of stars in a galaxy, because star formation effects dominate in the blue portion of the spectrum. To determine the stellar mass of a galaxy, we require the mass-to-light ratio, Υ_*. Ideally, we would like to measure Υ_* directly by some dynamical means, such as the observations of the vertical stellar velocity dispersion (Bottema 1993). Lacking such detailed information for each galaxy, we follow the work outlined in MdB and de Jong (1996). Based on dynamical data and stellar population models (Bruzual & Charlot 1993), they determine that there is a factor of 2 spread in Υ_* in the B bandpass, but that in I there is only a modest variation (less than 10%). Following the analysis presented in de Jong (1996), we adopt a mean value of $\Upsilon_* = 1.7$, although we note that a recent set of spectroevolutionary models by Bell & de Jong (2001) suggests that M/L can vary by as much as a factor of 2 over the color range of the dwarfs presented here (see their Fig. 3).

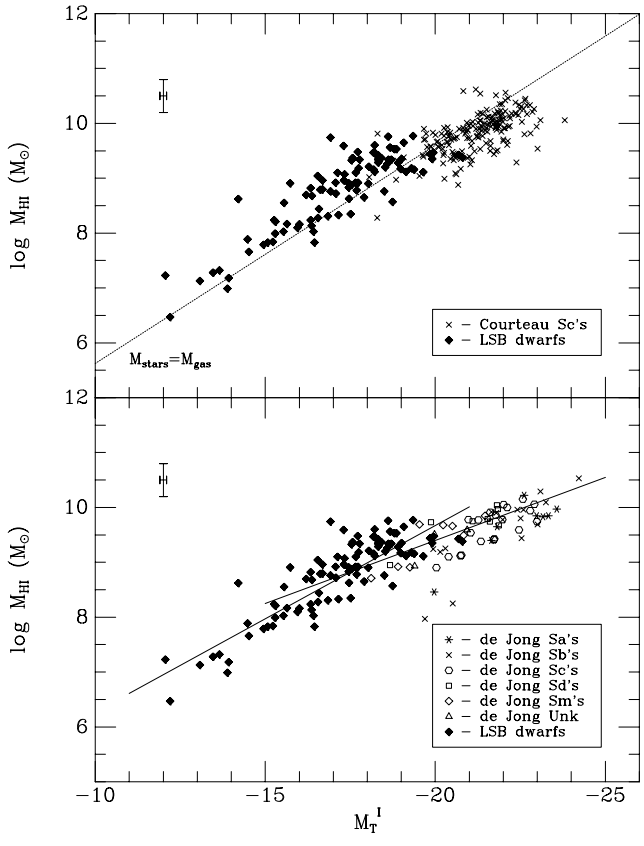

FIG. 3.—Total luminosity vs. H I gas mass for LSB dwarfs compared with Courteau Sc's (*top*) and de Jong spirals (*bottom*). The line of equal gas and stellar mass (assuming an M_*/L of 1.7 [McGaugh et al. 2000] and a conversion of H I to gas mass of 1.4) is shown in the top panel. The ordinary spirals display a shallower slope in the gas to stellar relationship, indicating that LSB dwarfs have been inefficient at converting their gas into stars.

The Courteau Sc sample is plotted with the LSB dwarfs in the top panel of Figure 3, and the de Jong spiral sample is plotted in the bottom panel. Also shown in the top panel is the equality line for gas and stellar mass, where the gas mass is determined from the H I mass after corrections for metals and nonatomic gas (see § 3.4). There has been no detection of CO emission from any LSB galaxy (Schombert et al. 1990; de Blok & van der Hulst 1998), so corrections for molecular gas are considered to be negligible (see Mihos, Spaans, & McGaugh 1999). For a majority of the disk galaxies in the de Jong and Courteau samples, the baryonic matter is in the form of stars, because their data points lie below the $M_{\rm stars} = M_{\rm gas}$ unity line. The opposite is true of the dwarfs, where a significant fraction of their baryonic matter is in the form of gas (primarily neutral hydrogen). Thus, the term "gas-rich" dwarf refers to this reversal, from stellar-mass dominance in disk galaxies to gas-mass dominance for the dwarf sequence.

The correlation between H I mass and total luminosity is not linear (in log space, i.e., different power-law slopes) for the whole range of galaxy luminosities. In fact, the dwarf sequence clearly has a steeper slope than both the de Jong spiral and the Courteau Sc samples. Linear fits to the three samples produce the following relations:

$$\log M_{\rm H\,I} = -0.22 M_T^I + 5.16 \text{ (Courteau Sc's)} ,$$

$$\log M_{\rm H\,I} = -0.23 M_T^I + 4.80 \text{ (de Jong disks)} ,$$

$$\log M_{\rm H\,I} = -0.34 M_T^I + 2.87 \text{ (LSB dwarfs)} ,$$

where the fits to the disks and dwarfs are shown in the bottom panel of Figure 3. The error in the slopes is ± 0.02. The de Jong spirals are slightly more gas-massive than the Sc sample at the low-luminosity end, in agreement with the findings of de Blok, McGaugh, & van der Hulst (1996). Some adjustment might be necessary to the Sc sample, because Sc's contain a small fraction of their gas in molecular form (although this amount is very small; see Young and Knezek 1989).

Assuming that M_*/L does not systematically change with $M_{\rm gas}$ between late-type disks and dwarfs, the relation between stellar and gas mass is given by $M_{\rm gas} \propto M_*^{0.55}$ for disks and $M_{\rm gas} \propto M_*^{0.88}$ for dwarfs. The shallower slope for disk galaxies implies that they have been more efficient at converting gas into stars in the past, assuming that all galaxies form from a single reservoir of gas. This also agrees with the previous observation that disk galaxies typically have a greater amount of their baryonic mass in stars rather than in gas. Interestingly, even the LSB spirals in de Jong's sample, which have different star-formation histories from other spirals in the sample, display the same gas-to-stellar-mass behavior as the Sc galaxies.

3.3. *Gas Fractions*

The standard measure of the gas-richness of a galaxy is their ratio of gas mass to luminosity, $M_{\rm H\,I}/L$. Figure 2 displays the distribution of $M_{\rm H\,I}/L$ for dwarfs versus the two spiral samples. The LSB dwarf sample has a higher mean $M_{\rm H\,I}/L$ (5 vs. 0.5 for disks), but there is a great deal of overlap between the samples. Note that many LSB dwarfs presented here have $M_{\rm H\,I}/L$ values greater than 5. This represents new extremes in gas-to-light ratio, because, for

example, none of the dwarfs studied by either van den Hoek et al. (2000) or van Zee, Haynes, & Salzer (1997) have $M_{\rm H\,I}/L$ values above 0.5 at I. More relevant is the trend of $M_{\rm H\,I}/L$ with luminosity (i.e., stellar mass) and central surface brightness (i.e., stellar density). These diagrams are shown in Figure 4 for the LSB dwarf and de Jong spiral samples. Whereas the trend of higher $M_{\rm H\,I}/L$ with lower luminosity in the de Jong disk galaxies continues to lower luminosities, the dwarf data, by themselves, are not as highly correlated as the disk galaxies.

The change in the relationship between $M_{\rm H\,I}/L$ and central surface brightness (μ_0^I) is particularly striking from the disks to dwarfs (Fig. 4, *top panel*). The previously tight correlation for ordinary spirals all but disappears for the dwarfs. However, the dwarfs do serve to fill the high-$M_{\rm H\,I}/L$, low-μ_0^I region of the diagram. In fact, the previous correlations may be mostly due to various boundary conditions imposed by our galaxy catalogs and to unfilled regions of the diagram that are empty for astrophysical reasons. For example, the sharp lower boundary may mark the limit placed by galactic winds from the first epoch of star formation. As the surface density of a galaxy drops (i.e., lower surface brightness), it becomes easier to eject its ISM because of heating by supernovae (Dekel & Silk 1986). Thus, the lower left region of the $M_{\rm H\,I}/L$-μ_0^I diagram would be inhabited by objects with neither sufficient gas (due to blowout) nor enough stars (due to a lack of gas for star formation) to be detected in the optical or radio (e.g., extremely LSB dwarf ellipticals). On the other hand, the upper right region of the diagram is an area that would be occupied by extremely bright, high H I mass galaxies. Such objects are expected to be short-lived, as they would be unstable in strong star formation events, converting all their gas into stars and thereby rapidly lowering their $M_{\rm H\,I}/L$ value.

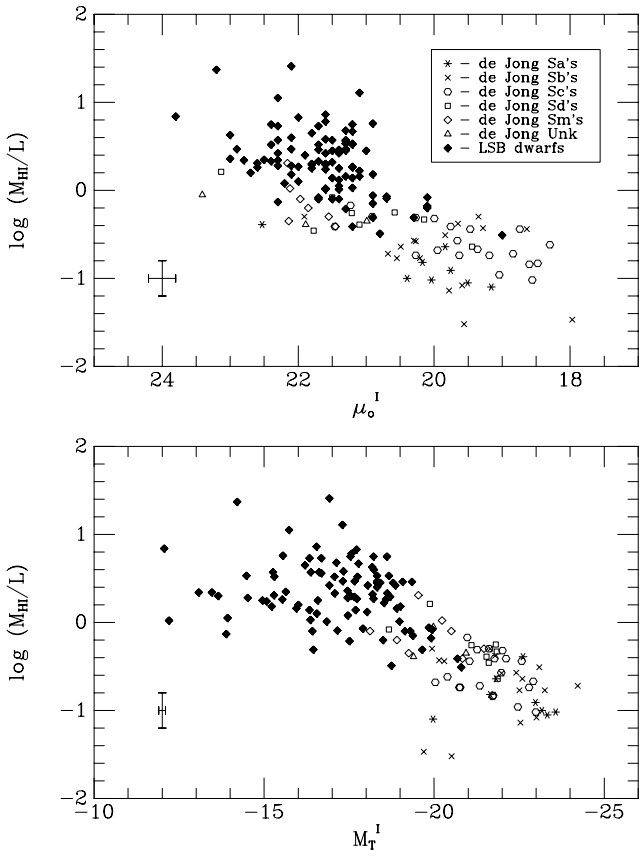

FIG. 4.—Gas-to-light ratios ($M_{\rm H\,I}/L$) vs. total luminosity and surface brightness. The previously strong correlations for disk galaxies are extended by LSB dwarfs, but the LSB dwarfs are not as well correlated by themselves.

The $M_{\rm H\,I}/L$ values can also be used to determine the gas fraction in a galaxy. As outlined by MdB, the baryonic gas mass fraction is given by

$$f_g = \frac{M_g}{M_g + M_*},$$

where M_g is the total mass in the form of gas (neutral, ionized, and metals), and M_* is the mass in stars. To relate these to the H I observations, we need the stellar mass-to-light ratio ($M_* = \Upsilon_* L$) and the amount of gas represented by neutral hydrogen ($M_g = \eta M_{\rm H\,I}$). The parameter η plays a role for the gas analogous to that played by Υ_* for stars and accounts for helium, metals, and gas phases other than atomic hydrogen. With these definitions, it is straightforward to obtain

$$f_g = \left(1 + \frac{\Upsilon_* L}{\eta M_{\rm H\,I}}\right)^{-1}.$$

Following the analysis presented in McGaugh et al. (2000), we adopt their mean value of $\Upsilon_* = 1.7$.

For the gas, η must be corrected for both the hydrogen mass fraction X and the phases of gas other than atomic hydrogen. We assume a solar hydrogen mass fraction, giving $\eta = X_\odot^{-1} = 1.4$. Variations in helium and metal content result in deviations from this value of less than 10%. This is a very small effect compared to that of other gas phases. Ionized gas in H I regions and hotter plasma is of negligible mass in late-type galaxies. In addition, molecular gas is also negligible for galaxy types later than Sc (Young & Knezek 1989), and there has been no detectable CO emission in LSB galaxies (Schombert et al. 1990). Therefore, we adopt the solar hydrogen mass fraction of 1.4 for η.

The histograms of gas fraction f_g for the LSB dwarf and comparison disk samples are shown in Figure 2. The gas fractions display behavior similar to that of the H I mass distributions. A majority of the galaxies in the disk samples have f_g values below 0.5, whereas the dwarf galaxies have very high f_g values, many objects reaching an unprecedented 90% in gas fraction. In the disk samples, the f_g values peaked at 0.3, but in the dwarf sample over 90% of the galaxies have f_g greater than 0.3. Note that the high f_g values for LSB dwarfs imply that there has been no epoch of baryonic blowout such as has been found for early-type galaxies (Bothun, Eriksen, & Schombert 1994; Mac Low & Ferrara 1999), unless there has been gas replenishment by infall, an unlikely prospect given the low dynamical masses of these systems (Eder & Schombert 2000). Adjusting the Υ_* for the bluer colors of LSB dwarfs would increase, on average, the calculated f_g, making their distribution even more extreme compared with that of disks.

The relationship between gas fraction and the optical properties of a dwarf galaxy is not as strong as that for disk galaxies, but several trends are clear. Lower luminosity and low surface brightness (lower stellar density) dwarf galaxies have much higher gas fractions than disk galaxies. Most dwarfs have higher gas fractions than either HSB or LSB disk galaxies (see Fig. 8 of MdB), yet lack the strong corre-

lation with luminosity or surface brightness that suggests a less orderly star formation history compared with disks. We interpret this trend as implying that LSB dwarfs are LSB simply because they have not converted their gas into stars with the same efficiency as either HSB or LSB disks.

To investigate this behavior further, we have adapted the chemical and spectrophotometric models from Boissier & Prantzos (2000, hereafter BP), who present predictions of gas fractions, surface brightness, and color for a range of galaxy masses. While intended to model disk galaxies, the BP models follow a cold dark matter framework and use scaling laws (Mo, Mao, & White 1998) that should be applicable to dwarf galaxies as well as to disks. The smallest masses in their models correspond to rotation values of 80 km s^{-1}, which is similar to the H I widths of the LSB dwarf sample.

A full description of the BP models can be found in their series of papers (see BP for references). Briefly, the models assemble a set of evolving rings to represent a galaxy formed by primordial infall. The CDM scenario for galaxy formation requires that the density fluctuations in the early universe give rise to dark matter–dominated halos. Within these halos, baryonic gas condenses to form disks. The resulting disks will have characteristic central densities, scale lengths, and masses in scalable terms, although these are not necessarily correlated, because a galaxy of a particular mass can form with a range of central surface brightnesses and sizes. BP introduce the spin parameter λ, relating halo mass and angular momentum as described by Mo et al. (1998), as the fundamental parameter to characterize and distinguish the various models.

Under this formalism, the spin parameter and circular velocity (effectively, the disk mass) determine the characteristic timescale for star formation. In addition, the model galaxies' structures are such that low-λ models ($\lambda = 0.01$) simulate HSB galaxies and high-λ models ($\lambda = 0.09$) have surface brightness profiles that recover the same structure as LSB dwarfs and disks. The simulations also allow the tracking of gas and stellar mass fractions as a function of time. By late epochs (13 Gyr; see Fig. 8 of BP), high-λ simulations have gas fractions between 0.6 and 0.8, similar to the values found for the LSB dwarfs in our sample. All this formalism is normalized to data for the Milky Way, thus completing the circle of structural and stellar population effects.

A comparison of the BP models (at time step 13 Gyr) with the LSB dwarf gas fractions and surface brightnesses is found in Figure 5. Each set of models for a specific spin parameter λ covers a range of gas fractions and central surface brightnesses. Each track (*solid line*) represents a single value of λ, where the brighter (lower f_g) edge of the tracks represents high-mass (high-V_c) models and the fainter edge corresponds to low-mass systems. As can be seen in Figure 5, the BP models predict the general trend of higher f_g with fainter μ_0. However, the models appears to be about 1 mag too bright, compared with the position of the LSB dwarfs and disks.

A similar disagreement between models and observations was noted in BP for the low surface brightness realm, and it seems clear that additional models with $\lambda > 0.1$ would begin to match the observed central surface brightnesses of LSB dwarfs. However, we note that age could also explain the discrepancy between models and observations. Low-mass, high-λ models typically brighten by 1 mag between 7 and 13 Gyr (because of an increasing SFR and continued conversion of gas mass into stellar mass). Thus, if LSB dwarfs were, on average, 5 Gyr younger than other disk galaxies, the models would exactly match the data. Color information confirms this interpretation, as will be discussed in the next section. Since the lower-λ models require decreasing star formation rates, then the surface brightness offset seen between the models and the disk data is probably due to a mismatch in the models to the accumulation of stellar mass relative to the Milky Way. Younger age is not an explanation for the disk systems, because decreasing star formation leads to a fading in surface brightness, the opposite of what is seen in Figure 5.

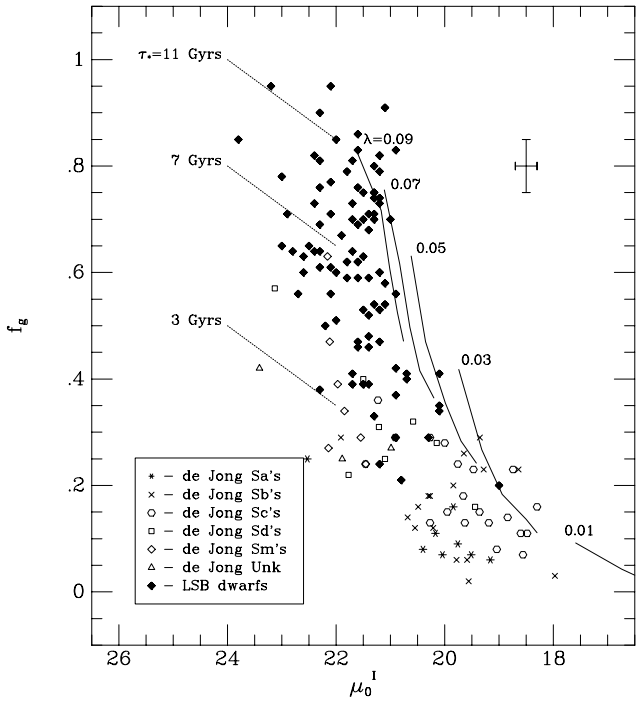

FIG. 5.—Central surface brightness (μ_0^I) vs. gas mass fraction (f_g). The data from de Jong for disk systems are shown by morphological type. LSB dwarfs (*filled diamonds*) are, typically, much higher in gas fraction. Also shown are the 13 Gyr galaxy evolution models of Boissier & Prantzos (2000). Each track follows the model gas fraction and surface brightness as a function of mass for various spin parameters, λ. High λ-values correspond to LSB systems, whereas low λ-values scale to normal disk galaxies. Lower f_g values on each track indicate the higher mass models, and the opposite edge is for galaxies with circular velocities of 80 km s^{-1}. While the models predict the observed f_g values for LSB dwarfs, the model surface brightnesses are 0.5–1 mag too bright. Under the model formalism, this would imply mean ages for the LSB dwarfs of 3–5 Gyr younger than the shown models. Also shown are tracks of *e*-folding star formation timescales (*dotted lines*) from the evolution models. LSB dwarfs display longer star formation timescales than disk systems.

The various BP models also map into star formation *e*-folding times (as given by Fig. 5 of BP) as a function of galaxy mass. Boundaries for star formation timescales of 11, 7, and 3 Gyr are also shown in Figure 5. As one would expect from their high gas fractions, LSB dwarfs typically lie in the region of the diagram occupied by galaxies with very long *e*-folding timescales. This would agree with their low metallicity values (McGaugh 1994; van Zee et al. 1997) and with their low current star formation rates, based on Hα imaging, and supports the conclusion that LSB dwarfs are slowly evolving systems.

3.4. *Colors*

The final clue to the star formation history of LSB dwarfs lies in their colors. Figure 6 displays the $V-I$ colors versus total luminosity (M_T^I), central surface brightness (μ_0^I), and gas fraction (f_g) for the LSB dwarfs and de Jong spirals. $V-I$ is chosen as the comparison color because it focuses on the mean color of the giant stars in a galaxy, a measure of the star formation in the last 5 Gyr, whereas a color index such as $B-V$ is a measure of contribution from massive stars (i.e., very recent star formation). This is an important distinction, because interpretation using the $V-I$ colors cannot discriminate between constant star formation over 5 Gyr or a series of short, weak bursts within that same time frame.

Several familiar trends are evident from Figure 6. One is that there is a clear tendency for galaxies to have bluer colors with lower surface brightness (*middle panel*). This pattern was first noted by Schombert et al. (1992) and has been studied by several authors (Gerritsen & de Blok 1999; Bell et al. 2000). Blue optical colors were of early importance, because they eliminated the fading hypothesis for the evolution of LSB galaxies (McGaugh & Bothun 1994; see O'Neil et al. 1997 for the discovery of red LSB galaxies). It is interesting to note that the scatter in the color diagrams is much less at I than in similar diagrams using B or V magnitudes (see McGaugh, Schombert, & Bothun 1995). This is because LSB galaxies, by definition, have low luminosity densities; the contrast due to recent star formation is thus extremely sharp in blue indices, whereas in the far-red the tendency is toward average color changes, as a result of short bursts of star formation.

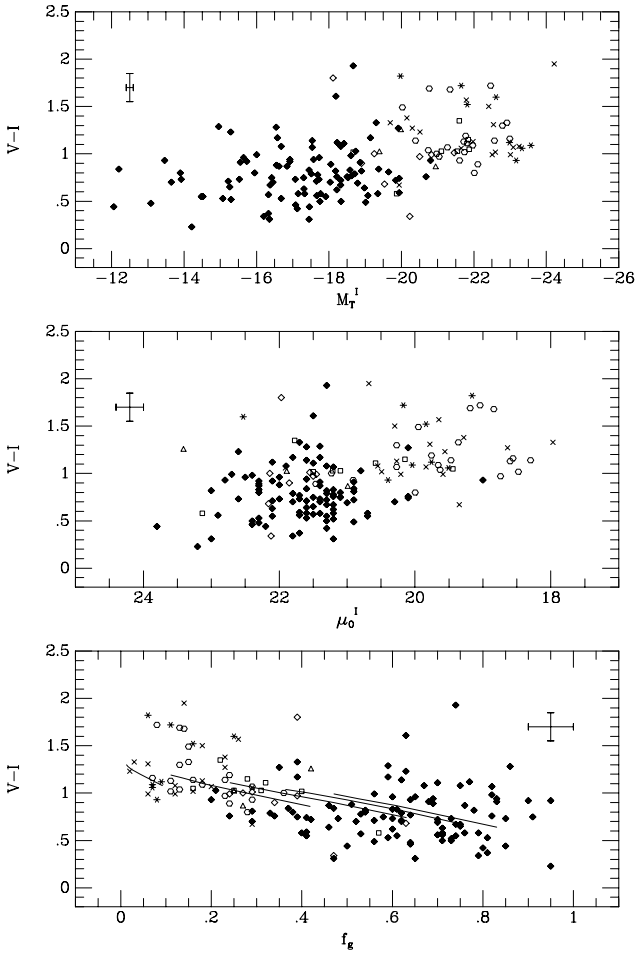

FIG. 6.—$V-I$ color vs. total luminosity (M_T^I, *top*), central surface brightness (μ_0^I, *middle*), and gas fraction (f_g, *bottom*). The LSB dwarfs continue the sequence, defined by ordinary spirals, of fainter luminosities, higher gas fractions, and lower surface brightnesses with bluer colors. The models of Boissier & Prantzos (2000) are shown in the bottom panel, where high λ-values (LSB) are to the right. Symbols are the same as in Fig. 5.

McGaugh & de Blok (1997) found a strong correlation between color and magnitude or surface brightness; however, despite the tendency for LSB galaxies to have blue optical colors, there is no direct correlation between $V-I$ and M_T^I or μ_0 for the LSB dwarf sample. On the other hand, the $(V-I)$-f_g relationship for LSB dwarfs is a clear extension of the relationships for disks from MdB. Interpretation of this trend is problematic. One might expect high-f_g galaxies to have inherently red colors, reflecting their low rate of gas mass conversion into stellar mass. The BP models are shown in the bottom panel of Figure 6, and they correctly predict the decrease in color with increasing gas fraction. This would seem to confirm several characteristics of the high-λ models, such as a rising star formation rate and slow chemical enrichment.

Also visible in Figure 6 is the fact that the dwarfs with the highest gas fractions have the bluest colors. Blue colors have always been an enigma in the understanding of LSB stellar populations. In general, the cause of the bluer colors in LSB galaxies, as compared with HSB galaxies, can be (1) low mean metallicity, (2) younger mean age, (3) a recent burst of star formation, or, of course, (4) some combination of the three. For example, van den Hoek et al. (2000) are able to reproduce the colors and gas fractions of LSB disks using an exponentially decreasing star formation model consistent with measured [O/H] values for their sample. However, they are unable to fit the bluest dwarf LSB galaxies in their sample without an additional light contribution from a younger stellar population.

Considering metallicity effects first, LSB galaxies are known to have lower metallicities than HSB galaxies, based on [O III] measurements of H II regions (McGaugh 1994; van Zee et al. 1997). These values range from 1/3 to 1/20 of solar, which corresponds to an [Fe/H] of -0.4 and -1.3 dex. While $V-I$ colors are not as sensitive to metallicity changes as color indices such as $B-V$, a shift of 1.0 dex in [Fe/H] will produce a change of 0.2 to the $V-I$ colors (G. Bruzual, A. & S. Charlot 2000, private communication). Thus, some of the blueward slope in the top panel of Figure 6 is due to a mean metallicity that decreases from approximately solar at high masses to 1/25 of solar at the faint end (Zaritsky 1993).

In order to examine the effects of metallicity, we have adapted the multimetallicity models for dwarf ellipticals from Rakos et al. (2001) to the color-magnitude relation in Figure 6. These models combine the metallicity distribution given by the Kodama & Arimoto (1997) infall simulations with the single-burst photometric models of Bruzual & Charlot (2000, private communication). For each metallicity bin in the Kodama & Arimoto model, the fraction of stars is calculated and the flux and color are determined from the Bruzual & Charlot single stellar populations. Then, the total integrated color of a galaxy is calculated by summing the luminosity of each metallicity bin population. To simulate the change of metallicity with mass, the shape of the Kodama metallicity distribution is held fixed, but the

peak [Fe/H] is compressed to lower values but constant fractions. This procedure successfully produces the correct slope and zero points of the color-magnitude relation for ellipticals (see Rakos et al. 2001 for a fuller discussion).

The resulting mass-metallicity relation for a 13 Gyr population, converted into I-band magnitudes and $V-I$ color, is shown in the top panel of Figure 7. The model fits the blue edge of the de Jong disk galaxies fairly well and is, of course, the mass-metallicity relation for spirals documented by Zaritsky, Kennicutt, & Huchra (1994). The number of disk galaxies above the 13 Gyr line probably represents systems with reddening due to dust. We also note that few LSB dwarfs display an indication of reddening, where the reddest LSB dwarfs are similar in $V-I$ color to dwarf ellipticals. This observation is in agreement with their lack of *IRAS* detection (Schombert et al. 1990), and van den Hoek et al. (2000) also rule out any significant extinction by dust in high gas fraction LSB galaxies.

While the color-magnitude relation works well for LSB disks, HSB spirals, and ellipticals, a majority of the LSB dwarf sample continue to have $V-I$ colors bluer than could be expected from their metallicities. Of course, it is possible that the stellar population that produces the optical luminosity has a much lower mean metallicity than that measured from nebular spectroscopy, because those values represent the current metallicity of ongoing star formation. However, the multimetallicity models take into account the contribution from metal-poor stars, and to achieve the $V-I$ colors observed for LSB dwarfs would require a contrived evolutionary history such that a majority of the stars have globular cluster metallicities with a recent, abrupt rise in the mean metallicity to match H II-region spectroscopy. Dominance by a globular cluster metallicity population certainly cannot be the case in all LSB dwarfs, because the galaxies with the highest $V-I$ values (the "red" edge in Fig. 7) follow the same mass-metallicity relation as disk and dwarf ellipticals (predicting mean metallicities of [Fe/H] = -0.8 from the models). If the blueward dwarfs are due to metallicity effects, then the mass-metallicity sequence breaks down below $M_T^I = -20$, an effect not indicated by LSB nebular spectroscopy (Bell et al. 2000).

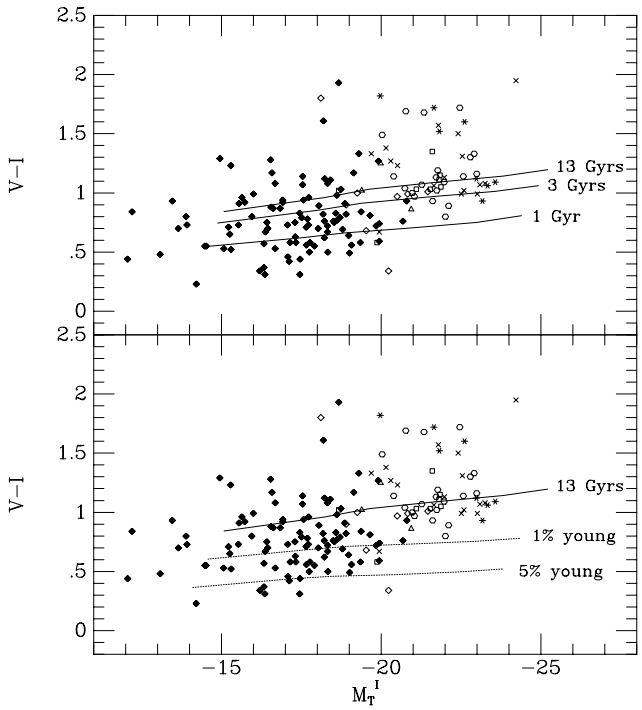

FIG. 7.—$V-I$ color vs. total luminosity (M_T^I). Symbols are the same as in Fig. 5. The top panel displays the multimetallicity models of Rakos et al. (2001) using the Bruzual & Charlot (2000, private communication) spectral energy distributions to convert to $V-I$ colors. Three population ages are shown; 13, 3, and 1 Gyr. A majority of LSB dwarfs have mean $V-I$ colors which concur with mean ages at least 10 Gyr less than normal ellipticals. The bottom panel displays two "frosting" models where a fraction of a recent (100 Myr) population is added to a 13 Gyr population. While only a 1% burst is required to match the colors of LSB dwarfs, this population would contribute 40% of the total light of the galaxy and eliminate its LSB appearance.

An alternative explanation is that the spread in $V-I$ color is due to changes in the mean age of the stellar population in LSB dwarfs. To test the effects of age, we have recomputed the luminosities and colors of the multimetallicity models for ages of 1 and 3 Gyr (shown in Fig. 7), where an initial burst of star formation less than 0.1 Gyr in duration is assumed. The $V-I$ colors evolve quickly, reaching the red edge in only 5–6 Gyr. If mean age is responsible for the bluer $V-I$ colors, then an age between 1 and 3 Gyr is indicated. This, of course, does not imply that LSB dwarfs formed less than 4 Gyr ago, since a young mean age can be achieved through a number of scenarios. For example, the BP models predict an increasing star formation rate with time in their high-λ, low-mass simulations. With e-folding timescales between 7 and 11 Gyr (as indicated by Fig. 7), then, a majority of the luminosity in LSB dwarfs originates with stars less than 3 Gyr old, even though there will exist stars dating back to the epoch of galaxy formation.

A younger mean age can also be produced by a burst of recent star formation on top of an underlying old population. Recent star formation can be tested for using so-called frosting models, where some percentage of young stars is added to a 13 Gyr population. The bottom panel of Figure 7 displays the effects of adding 1% and 5% of a 100 Myr population to the 13 Gyr mass-metallicity sequence. While a 5% young population is sufficient to match the $V-I$ colors of the LSB dwarfs in the color-magnitude diagram, a star formation burst of this magnitude is inconsistent with other properties of LSB galaxies. For example, the burst population in a 1% population contributes 40% of the total light of the galaxy, and in a 5% population this percentage rises to 80% of the total light. Given the slow rotation velocities for dwarfs, this young, bright population would maintain a tight spatial correlation, producing many high surface brightness knots, in contradiction with the visual appearance of the LSB dwarfs. In order to maintain a low stellar density and the lack of color gradient (Pildis et al. 1997), the young population would have to be evenly distributed instead of in cloud complexes, a style of star formation currently undocumented in extragalactic studies. In addition, even if the recent burst were spread evenly within the LSB dwarf, the burst strength is inconsistent with the current metallicities and gas fractions.

Lastly, the difference in $V-I$ colors between LSB dwarfs and disks may be due to the fact that disk systems have high amounts of dust extinction. Clearly, some of the disk colors in Figure 6 are reddened, particularly the objects with $1.5 \leq V-I \leq 2$. Half of the early-type disks have $V-I$ colors greater than 1.2, the red edge for the LSB dwarfs, while the rest of them appear to be less effected by extinc-

tion effects, with a blue edge for the disk sample near $V-I=1$. Tully et al. (1998) find that, in the extreme case of a sample of edge-on galaxies, extinction at I can reach 1 mag, which would correspond to 0.3 in $V-I$. However, studies of overlapping pairs of ellipticals and late-type galaxies by Domingue, Keel, & White (2000) find only modest amounts of extinction. The correlation of color-magnitude for disk galaxies near $V-I=1$ would argue that we are observing a majority of the optical luminosity in disk galaxies, unless extinction effects conspire to redden the mean colors into this linear relationship.

4. CONCLUSIONS

In this study we have isolated the optical and H I properties of a sample of LSB dwarf galaxies in order to study the relationship between gas fraction and star formation history. Our primary results can be summarized as follows.

1. Objects selected by irregular dwarflike morphology (to be distinguished from irregular tidal morphology) do indeed define a sample of galaxies that are faint, small, and low in mass (Pildis et al. 1997). However, no single characteristic defines a galaxy as uniquely dwarf or giant. There is a continuum of optical properties, such as central surface brightness, luminosity, and scale length, over the range of galaxy Hubble types (Fig. 1).

2. The distribution of H I mass is such that the typical LSB dwarf has less than $(5 \times 10^9)\ M_\odot$ of neutral gas (Fig. 2). Over one-third of the dwarfs in this sample have H I mass less than $(5 \times 10^8)\ M_\odot$. A galaxy defined by irregular morphology will be a dwarf not only in size and luminosity, but also in H I mass and dynamical mass (Eder & Schombert 2000).

3. There is a relationship between stellar mass and gas mass for both dwarf and disk galaxies (Fig. 3). However, the relation for dwarfs is much shallower than the relation for disks, implying that disks have been more efficient at converting gas into stars in the past (Bell & de Jong 2000). This is in line with the more ordered appearance of disks, versus the chaotic structure of dwarfs, but this conclusion is dependent on there being only small variations in M/L between late-type disks and dwarfs, which may not be the case (see Bell & de Jong 2001).

4. LSB dwarfs typically have much higher gas fractions (the ratio of stellar to gas mass) than do disk galaxies (Fig. 2). Many of the simple correlations in disk galaxies between gas fraction and luminosity or surface brightness are weaker in the dwarf realm. LSB dwarfs with the bluest colors have the highest gas fractions (Fig. 6).

The gas mass fraction of a galaxy must be a key parameter of its evolutionary path, because the pattern, duration, and strength of star formation are directly determined by the amount of fuel available to support star formation. Disk galaxies, with red underlying stellar populations and low gas fractions, suggest a star formation history that involves constant or declining star formation at relatively high rates (Bell & de Jong 2000; van den Hoek et al. 2000). Under this scenario, the gas fraction becomes a gauge of integrated past conversion of gas into stars. Thus, the Hubble sequence is a progression of star formation rates, where Sa's have the highest rates and, in the present epoch, the lowest gas fractions and Sc's have lower rates and maintain higher gas fractions.

For LSB dwarfs, the global characteristics are the reverse of those of ordinary spirals. They have very little in the way of a stellar population, and a majority of their baryonic mass is in the form of neutral hydrogen. The stellar population that does exist is very low in surface density and very blue, based on their $V-I$ colors (Pildis et al. 1997). Using the prescription from van Zee et al. (1997), their integrated past star formation rate is typically less than $0.1\ M_\odot\ \mathrm{yr}^{-1}$, and H$\alpha$ imaging of a few LSB dwarfs indicates current star formation rates of $0.01\ M_\odot\ \mathrm{yr}^{-1}$. On the other hand, their gas mass fractions are very high, greater on average than that of the typical Sc galaxy. Combining their current colors and star formation properties with the knowledge that their metallicities are low (1/3 to 1/20 of solar), LSB dwarfs must represent unevolved systems that have consumed very little of their original gas supply, in agreement with the van Zee et al. (1997) study of gas-rich dwarfs.

Our comparison with simple photometric–gas consumption models presented in § 3.3 (displayed in Fig. 5) provides the key difference in the characteristics of dwarfs and disks. Disk galaxies, over a range of central surface brightnesses, have used a significant fraction of their gas to produce stars (see also Bell & de Jong 2000). They have short star formation e-folding times, but they display relatively old mean stellar ages, reflecting a long history of substantial star formation. Dwarfs, on the other hand, have consumed very little of their gas, because of their long star formation timescales, and their current, dominant stellar population has a very young age (less than 5 Gyr on average).

Young mean age, achieved by either constant or increasing star formation, appears to be the most likely solution to the optical colors presented in Figure 7. With the levels of star formation deduced for the integrated past or for the observed current, it is difficult to envision star formation spread evenly in time and spatial position. More likely, star formation in LSB dwarfs proceeds in weak bursts that percolate over the spatial extent of the galaxies, with each event consuming only a small fraction of the local H I gas mass. This hypothesis of weak bursts on top of a very LSB stellar population is in agreement with Hα studies of LSB galaxies (Walter & Brinks 1999), where star formation traces both the gas and the surface brightness, and it is also in agreement with the conclusions of Bell et al. (2000), who found a strong correlation between an LSB galaxy's star formation history and its local surface density.

We conclude with a comment on the differences between LSB dwarf galaxies and LSB disk galaxies. The star formation history of LSB disk galaxies has recently been explored by both Bell et al. (2000) and van den Hoek et al. (2000). The latter authors find that LSB disks have gas fractions lower than those of the LSB dwarfs presented here, though still higher than those of HSB disk galaxies (e.g., f_g around 0.5). They find that exponentially decreasing SFR models are a good match to most LSB disk properties; however, weak bursts are indicated for the bluest systems. Bell et al. (2000) find similar results, with the additional correlation between local surface brightness (mass density) and past-plus-current star formation rate. Both studies find that LSB disks are lower in mean age than HSB disks, mostly because of the more rapid buildup of a stellar population in HSB with higher past rates of star formation. In other words, a higher surface brightness system has more old stars per square parsec and, thus, its calculated mean age from model comparison is older. LSB dwarfs have many characteristics

in common with LSB disks, but the star formation history cannot be as smooth and uniform as proposed by Bell et al. (2000) and van den Hoek et al. (2000) for LSB disks. The correlations found by MdB for disks are much weaker for LSB dwarfs, signaling a difference in the style of star formation even within the class of LSB galaxies. We suspect that the dynamical state of disks, versus that of dwarfs, is responsible for the changes seen in their stellar and gas properties as a galaxy makes the transition from ordered rotation to the more turbulence-dominated solid-body rotation found in dwarfs (see van Zee et al. 1997). However, that conclusion remains in question until high-resolution H I mapping of LSB dwarfs is presented in a future paper.

We wish to thank the generous support of the Arecibo Observatory for the allocation of time to search for H I emission from the candidate dwarf galaxies and of the MDM Observatory in carrying out the photometry portion of this program. This work is based on photographic plates obtained at the Palomar Observatory 48 inch (1.2 m) Oschin Telescope for the Second Palomar Observatory Sky Survey, which was funded by the Eastman Kodak Company, the National Geographic Society, the Samuel Oschin Foundation, the Alfred Sloan Foundation, the National Science Foundation, and the National Aeronautics and Space Administration.

REFERENCES

Ashman, K. 1992, PASP, 104, 1109
Baugh, C. M., Cole, S., & Frenk, C. S. 1996, MNRAS, 283, 1361
Bell, E. F., Barnaby, D., Bower, R. G., de Jong, R. S., Harper, D. A., Jr., Hereld, M., Loewenstein, R. F., & Rauscher, B. J. 2000, MNRAS, 312, 470
Bell, E. F., & de Jong, R. S. 2001, ApJ, 550, 212
———. 2000, MNRAS, 312, 497
Boissier, S. & Prantzos, N. 2000, MNRAS, 312, 398 (BP)
Bothun, G. D., Eriksen, J., & Schombert, J. M. 1994, AJ, 108, 913
Bottema, R. 1993, A&A, 275, 16
Bruzual A., G., & Charlot, S. 1993, ApJ, 405, 538
Carignan, C., & Purton, C. 1998, ApJ, 506, 125
Courteau, S. 1996, ApJS, 103, 363
de Blok, W. J. G., McGaugh, S. S., & van der Hulst, J. M. 1996, MNRAS, 283, 18
de Blok, W. J. G., & van der Hulst, J. M. 1998, A&A, 336, 49
de Jong, R. S. 1996, A&A, 313, 45
Dekel, A., & Silk, J. 1986, ApJ, 303, 39
Domingue, D. L., Keel, W. C., & White, R. E., III 2000, ApJ, 545, 171
Driver, S., & Cross, N. 2000, in ASP Conf. Ser. 218, Mapping the Hidden Universe, ed. R. C. Kraan-Korteweg, P. A. Henning, & H. Andernach (San Francisco: ASP)
Driver, S. P., Windhorst, R. A., & Griffiths, R. E. 1995, ApJ, 453, 48
Eder, J., Oemler, A., Jr., Schombert, J. M., & Dekel, A. 1989, ApJ, 340, 29
Eder, J., & Schombert, J. M. 2000, ApJS, 131, 47
Gerritsen, J. P. E., & de Blok, W. J. G. 1999, A&A, 342, 655
Giovanelli, R., & Haynes, M. P. 1988, in Galactic and Extragalactic Radio Astronomy, ed. G. L. Verschuur & K. I. Kellermann (2d ed.; New York: Springer), 522
Impey, C. D., Sprayberry, D, Irwin, M. J., & Bothun, G. D. 1996, ApJS, 105, 209
Kodama, T., & Arimoto, N. 1997, A&A, 320, 41
Lake, G. 1990, ApJ, 364, L1
Matthews, L. D., van Driel, W., & Gallagher, J. S., III 1998, AJ, 116, 1169
Mac Low, M.-M., & Ferrara, A. 1999, ApJ, 513, 142
McGaugh, S. S. 1994, ApJ, 426, 135
McGaugh, S. S., & Bothun, G. D. 1994, AJ, 107, 530
McGaugh, S. S., & de Blok, W. J. G. 1997, ApJ, 481, 689 (MdB)
McGaugh, S. S., Schombert, J. M., & Bothun, G. D. 1995, AJ, 109, 2019
McGaugh, S. S., Schombert, J. M., Bothun, G. D., & de Blok, W. J. G. 2000, ApJ, 533, L99
Mihos, J. C., Spaans, M., & McGaugh, S. S. 1999, ApJ, 515, 89
Mo, H. J, Mao, S., & White, S. D. M. 1998, MNRAS, 295, 319
Patterson, R. J., & Thuan, T. X. 1996, ApJS, 107, 103 (PT)
Pildis, R. A., Schombert, J. M., & Eder, J. 1997, ApJ, 481, 157
O'Neil, K., Bothun, G. D., Schombert, J. M., Cornell, M. E., & Impey, C. D. 1997, AJ, 114, 2448
Rakos, K. D., Odell, A. P., & Schombert, J. M. 1997, ApJ, 490, 194
Rakos, K., Schombert, J., Maitzen, H. M., Prugovecki, S., & Odell, A. 2001, AJ, in press
Reid, I. N., et al. 1991, PASP, 103, 661
Schade, D., Lilly, S. J., Le Fèvre, O., Hammer, F., & Crampton, D. 1996, ApJ, 464, 79
Schneider, S. E., & Schombert, J. M. 2000, ApJ, 530, 286
Schneider, S. E., Spitzak, J. G., & Rosenberg, J. L. 1998, ApJ, 507, L9
Schombert, J. M., & Bothun, G. D. 1988, AJ, 95, 1389
Schombert, J. M., Bothun, G. D., Impey, C. D., & Mundy, L. G. 1990, AJ, 100, 1523
Schombert, J. M., Bothun, G. D., Schneider, S. E., & McGaugh, S. S. 1992, AJ, 103, 1107
Schombert, J. M., Pildis, R. A., & Eder, J. 1997, ApJS, 111, 233
Schombert, J. M., Pildis, R. A., Eder, J., & Oemler, A., Jr. 1995, AJ, 110, 2067
Tully, R. B., Pierce, M. J., Huang, J.-S., Saunders, W., Verheijen, M. A. W., & Witchalls, P. T. 1998, AJ, 115, 2264
van den Hoek, L. B., de Blok, W. J. G., van der Hulst, J. M., & de Jong, T. 2000, A&A, 357, 397
van Zee, L., Haynes, M. P., & Salzer, J. J. 1997, AJ, 114, 2479
Walter, F., & Brinks, E. 1999, AJ, 118, 273
Worthey, G. 1994, ApJS, 95, 107
Young, J. S., & Knezek, P. M. 1989, ApJ, 347, L55
Zaritsky, D. 1993, PASP, 105, 1006
Zaritsky, D., Kennicutt, R. C., Jr., & Huchra, J. P. 1994, ApJ, 420, 87
Zwaan, M. A., Briggs, F. H., Sprayberry, D., & Sorar, E. 1997, ApJ, 490, 173